12-22-2000

Layered Analytical Radiative Transfer Model For Simulating Water Color Of Coastal Waters And Algorithm Development

Charles R. Bostater Jr.

Lisa H. Huddleston

PROCEEDINGS OF SPIE

SPIEDigitalLibrary.org/conference-proceedings-of-spie

Layered analytical radiative transfer model for simulating water color of coastal waters and algorithm development

Charles R. Bostater
Lisa H. Huddleston

SPIE.

Layered analytical radiative transfer model for simulating water color of coastal waters and algorithm development

Charles R. Bostater, Jr.*, Lisa Huddleston
Marine Environmental Optics Laboratory & Remote Sensing Center
College of Engineering
Florida Tech

ABSTRACT

A remote sensing reflectance model, which describes the transfer of irradiant light within a homogeneous water column has previously been used to simulate the nadir viewing reflectance just above or below the water surface by Bostater, et al. [1,2,3]. Wavelength dependent features in the water surface reflectance depend upon the nature of the downwelling irradiance (direct & indirect), bottom reflectance (in optically shallow waters) and the water absorption and backscatter coefficients. The latter are very important coefficients, and depend upon the constituents in water and both vary as a function of the water depth and wavelength in actual water bodies. This paper describes a preliminary approach for the analytical solution of the radiative transfer equations in a two- stream representation of the irradiance field with variable coefficients due to the depth dependent water concentrations of substances such as chlorophyll pigments (chlorophyll-a), dissolved organic matter (DOM) and suspended particulate matter (seston). The analytical model formulation makes use of analytically based solutions to the 2-flow equations[1,2,3]. However, in this paper we describe the use of the unique Cauchy boundary conditions previously used, along with a matrix solution to allow for the prediction of the synthetic water surface reflectance signatures within a nonhomogeneous medium (a hypothetical water column defined by a variable water column layer depth and associated depth dependent concentrations of substances with unique layer characteristics). Observed reflectance signatures as well as model derived "synthetic signatures" are processed using efficient algorithms which demonstrate the error induced using the layered matrix approach is much less than 1% when compared to the analytical homogeneous water column solution. The influence of vertical gradients of water constituents may be extremely important in remote sensing of coastal water constituents as well as in remote sensing of submerged targets and different bottom types such as corals, sea grasses and sand.

Keywords: reflectance spectroscopy, remote sensing, radiative transfer, absorption coefficients, environmental models, environmental surveillance, hyperspectral remote sensing, environmental optics, water surface reflectance, water quality, inhomogeneous media radiative transfer models, bottom reflectance.

1. BACKGROUND

When we speak of radiative transfer models we generally are referring to forms of the radiative transfer equations similar to that given below. For example, a version of a radiative transfer equation and associated role of the absorption and scattering processes is described by Priesendorfer[4] in terms of a radiative transfer equation (RTE):

$$\mu \frac{dL(z;\xi;\lambda)}{dz} = -c(z;\lambda)L(z;\xi;\lambda) + \int_{\Xi} L(z;\xi';\lambda)\beta(z;\xi' \to \xi;\lambda)d\Omega(\xi') + \beta(z;\xi' \to \xi;\lambda)L_c(z;\xi) \quad ,(1)$$

where μ=cos θ (cosine of zenith angle), L is radiance ($Wm^{-2}sr^{-1}$), z depth (m) positive down, ξ is direction of light, λ represents wavelength (nm), c is a beam attenuation coefficient (absorption + scattering) (m^{-1}), Ξ indicates integration over directions of a unit sphere, β is a volume scattering function[5] ($m^{-1}sr^{-1}$) which describes the amount of light originally heading in direction ξ' at depth z elastically scattered into direction ξ (elastic scattering is used to denote scattering with no change of wavelength, whereas inelastic scattering is that scattering process which involves a change of wavelength or frequency). L_c is the collimated radiance ($Wm^{-2}sr^{-1}$).

---

* Correspondence: Dr. Charles Bostater, 150 West Univ. Blvd., Melbourne FL., USA, email: bostater@probe.ocn.fit.edu http://www.ocn.fit.edu ph: 321-258-9134 (Fax) 321-773-0980.

The first term on the right hand side of 1 is the loss of radiant energy from due to ***absorption*** and **scattering (backwards or forwards)** out of the path of the radiant energy flux. The 2nd and 3rd terms are gains due to the collimated or a path radiance being scattered within the path of the radiant energy (either diffuse or collimated). Analytical models derived from the above (see the 2 flow equations below) have been solved and results demonstrated using Monte Carlo[6,7] techniques (Bostater and Gimond[8], Bostater[9]. The above RTE equation has been simplified into more readily solvable systems of differential equations, as witnessed in the well know versions of the two-flow equations[10] given below. A form of these equations have been given[1,2,3,4,10] by a set of two or three coupled ordinary differential equations that describe the upwelling and downwelling irradiance in a unit volume of water of depth z. The terms are a(λ), the absorption coefficient (m^{-1}), b(λ) is a backscatter coefficient (m^{-1}), $E_u(\lambda)$ is the upwelling irradiance (Wm^{-2}), $E_d(\lambda)$ is the downwelling irradiance (Wm^{-2}), and $R(\lambda)=E_u(\lambda)/E_d(\lambda)$ is the irradiance reflectance and c(λ) is a conversion coefficient. Below, we clearly show how a medium (such as water, a plant canopy, leaves or other tissue mediums, or a gaseous atmosphere) with measured or estimated absorption spectra, a(λ) and calculated backscatter spectra, b(λ), are utilized to solve for and predict a surface reflectance. The predicted signatures and solutions can then be used for algorithm development[11] that may include using numerical higher order derivative spectroscopy procedures[11]. Similar equations and solutions for different water types or classes have been utilized in marine and environmental optics[12,13,14,15].

The above type of solutions and those given below are needed in order to improve operational advances in the use of hyperspectral imagery for oceanographic and atmospheric models, environmental surveillance, agriculture, medical and earth system science management.

2. METHODS

The 2-flow equations are solved and preliminary results shown following the procedures below where the principle equations are given by:

$$\frac{dE_d^w}{dz} = -(a+b)E_d^w(z) + bE_u^w(z) + cE_s^w(z) \qquad (1.1)$$

$$\frac{dE_u^w}{dz} = (a+b)E_u^w(z) - bE_d^w(z) - cE_s^w(z) \qquad (1.2)$$

$$\frac{dE_s^w}{dz} = -\alpha E_s^w(z) \qquad (1.3)$$

Final solutions after applying Cauchy type boundary conditions are:

$$E_d^w(i) = X(i)\left(\frac{E_d^w(i-1) - m(i)}{2}\right) + Y(i)\left(\frac{\beta_d(i-1) + \alpha(i)m(i)}{2\psi(i)}\right) + m(i)e^{-\alpha(i)z(i)} \qquad (1.4)$$

$$E_u^w(i) = X(i)\left(\frac{E_u^w(i-1) - n(i)e^{-\alpha(i)z(i)}}{2}\right) + Y(i)\left(\frac{\beta_u(i) + \alpha(i)n(i)e^{-\alpha(i)z(i)}}{2\psi(i)}\right) + n(i) \qquad (1.5)$$

$$\beta_d(i-1) = -(a(i)+b(i))E_d^w(i-1) + b(i)E_u^w(i-1) + c(i)E_s^w(i-1) \qquad (1.6)$$

$$\beta_u(i) = (a(i)+b(i))E_u^w(i+1) - b(i)E_d^w(i+1) - c(i)E_s^w(i+1) \qquad (1.7)$$

where, i = layer number, z= depth of layer and the layered coefficients are assumed initially as:

$$c(i) = 2.52b(i) \tag{1.8}$$

$$\alpha(i) = a(i) + 53b(i) \tag{1.9}$$

$$\psi\text{(i)}=\sqrt{a(i)^2 + 2a(i)b(i)} \tag{1.10}$$

$$X(i) = e^{\psi(i)z(i)} + e^{-\psi(i)z(i)} \tag{1.11}$$

$$Y(i) = e^{\psi(i)z(i)} - e^{-\psi(i)z(i)} \tag{1.12}$$

$$m(i) = \frac{-c(i)(\alpha(i) + a(i) + 2b(i))}{\alpha(i)^2 - \psi(i)^2} E_s^w(i-1) \tag{1.13}$$

$$n(i) = \frac{c(i)(\alpha(i) - a(i) - 2b(i))}{\alpha(i)^2 - \psi(i)^2} E_s^w(i-1) \tag{1.14}$$

and we have used the assumed solution:

$$E_s^w(i) = E_s^w(i-1)e^{\alpha(i)z(i)} \tag{1.15}$$

Substituting equation (1.6) into equation (1.4) we get:

$$\begin{aligned} E_d^w(i) &= X(i)\left(\frac{E_d^w(i-1) - m(i)}{2}\right) \\ &+Y(i)\left(\frac{(-(a(i)+b(i))E_d^w(i-1) + b(i)E_u^w(i-1) + c(i)E_s^w(i-1))(+\alpha(i)m(i)}{2\psi(i)}\right) + m(i)e^{-\alpha(i)z(i)} \end{aligned} \tag{1.16}$$

Combining like terms of equation 1.16,one obtains:

$$\begin{aligned} E_d^w(i) &= E_d^w(i-1)\left(\frac{X(i)}{2} - \frac{a(i)Y(i)}{2\psi(i)} - \frac{b(i)Y(i)}{2\psi(i)}\right) + E_u^w(i-1)\left(\frac{b(i)Y(i)}{2\psi(i)}\right) \\ &+E_s^w(i-1)\left(\frac{c(i)Y(i)}{2\psi(i)}\right) - \frac{X(i)m(i)}{2} + \frac{\alpha(i)Y(i)m(i)}{2\psi(i)} + m(i)e^{-\alpha(i)z(i)} \end{aligned} \tag{1.17}$$

In order to set up preliminary terms for a matrix solution, the following preliminary approach is used:

$$\text{Let } D1(i) = \frac{\text{X(i)}}{2} - \frac{a(i)Y(i)}{2\psi(i)} - \frac{b(i)Y(i)}{2\psi(i)} \tag{1.18}$$

$$\text{Let } D2(i) = \frac{b(i)Y(i)}{2\psi(i)} \tag{1.19}$$

$$\text{Let } D3(i) = \frac{c(i)Y(i)}{2\psi(i)} \tag{1.20}$$

$$\text{Let } D4(i) = \frac{-m(i)X(i)}{2} + \frac{\alpha(i)m(i)Y(i)}{2\psi(i)} + m(i)e^{-\alpha(i)z(i)} \tag{1.21}$$

Substituting equations (1.18), (1.19), (1.20), and (1.21) into equation (1.17), we get:

$$E_d^w(i) = E_d^w(i-1)D1(i) + E_u^w(i-1)D2(i) + E_s^w(i-1)D3(i) + D4(i) \tag{1.22}$$

One performs the same operations for the upwelling equation, or substituting equation (1.7) into equation (1.5), one obtains:

$$\begin{aligned} E_u^w(i-1) &= X(i)\left(\frac{E_u^w(i) - n(i)e^{-\alpha(i)z(i)}}{2}\right) \\ &+Y(i)\left(\frac{((a(i)+b(i))E_u^w(i) - b(i)E_d^w(i) - c(i)E_s^w(i)) + \alpha(i)n(i)e^{-\alpha(i)z(i)}}{2\psi(i)}\right) + n(i) \end{aligned} \tag{1.23}$$

and combining like terms for equation (1.23), one obtains:

$$\begin{aligned} E_u^w(i-1) &= E_u^w(i)\left(\frac{X(i)}{2} + \frac{a(i)Y(i)}{2\psi(i)} + \frac{b(i)Y(i)}{2\psi(i)}\right) - E_d^w(i)\left(\frac{b(i)Y(i)}{2\psi(i)}\right) \\ &-E_s^w(i)\left(\frac{c(i)Y(i)}{2\psi(i)}\right) - \frac{X(i)n(i)e^{-\alpha(i)z(i)}}{2} + \frac{\alpha(i)Y(i)n(i)e^{-\alpha(i)z(i)}}{2\psi(i)} + n(i) \end{aligned} \tag{1.24}$$

In order to set up terms for matrix:

$$\text{Let U1}(i) = \frac{\text{X(i)}}{2} + \frac{a(i)Y(i)}{2\psi(i)} + \frac{b(i)Y(i)}{2\psi(i)} \tag{1.25}$$

$$\text{Let } D2(i) = \frac{b(i)Y(i)}{2\psi(i)} \tag{1.26}$$

$$\text{Let } D3(i) = \frac{c(i)Y(i)}{2\psi(i)} \tag{1.27}$$

$$\text{Let U4}(i) = \frac{-X(i)n(i)e^{-\alpha(i)z(i)}}{2} + \frac{\alpha(i)Y(i)n(i)e^{-\alpha(i)z(i)}}{2\psi(i)} + n(i) \tag{1.28}$$

and substituting equations (1.25), (1.26), (1.27), and (1.28) into equation (1.24), we get:

$$E_u^w(i-1) = E_u^w(i)U1(i) - E_d^w(i)D2(i) - E_s^w(i)D3(i) + U4(i) \tag{1.29}$$

where, at the bottom layer, we have a final equation:

$$E_u^w(k) = R_b E_d^w(k) + R_b E_s^w(k) \tag{1.30}$$

where k = bottom layer and R_b is the bottom reflectance and is also wavelength dependent. With equations (1.22), (1.29) and (1.30), we can write a system of linear equations in the form of $AX = B$ where Matrix A is an N by N matrix containing the coefficients of the linear system (input), B is a vector of length N containing the right-hand side of the linear system (input), and X is a vector of length N containing the solution to the linear system (output). The input matrix (Matrix A) is set up as follows:

$$\begin{bmatrix}
1 & 0 & 0 & 0 & 0 & \dots & 0 & 0 & 0 & 0 & -D2(1) \\
-D1(1) & 1 & 0 & 0 & 0 & \dots & 0 & 0 & 0 & -D2(2) & 0 \\
0 & -D1(3) & 1 & 0 & 0 & \dots & 0 & 0 & -D2(3) & 0 & 0 \\
\dots & \dots & \dots & \dots & \dots & \dots & \dots & \dots & \dots & \dots & \dots \\
0 & 0 & 0 & -D1(k) & 1 & 0 & -D2(k) & 0 & 0 & 0 & 0 \\
0 & 0 & 0 & 0 & -R_b & 1 & 0 & 0 & 0 & 0 & 0 \\
0 & 0 & 0 & 0 & D2(k) & -U1(k) & 1 & 0 & 0 & 0 & 0 \\
\dots & \dots & \dots & \dots & \dots & \dots & \dots & \dots & \dots & \dots & \dots \\
0 & 0 & D2(3) & 0 & 0 & \dots & 0 & -U1(3) & 1 & 0 & 0 \\
0 & D2(2) & 0 & 0 & 0 & \dots & 0 & 0 & -U1(2) & 1 & 0 \\
D2(1) & 0 & 0 & 0 & 0 & \dots & 0 & 0 & 0 & -U1(1) & 1
\end{bmatrix} \tag{1.31}$$

The B vector is set up as follows:

$$\begin{bmatrix}
D1(1)E_d^w(0) + D3(1)E_s^w(0) + D4(1) \\
D3(2)E_s^w(1) + D4(2) \\
D3(3)E_s^w(2) + D4(3) \\
\dots \\
D3(k)E_s^w(k-1) + D4(k) \\
R_b E_s^w(k) \\
U4(k) - D3(k)E_s^w(k) \\
\dots \\
U4(3) - D3(3)E_s^w(3) \\
U4(2) - D3(2)E_s^w(2) \\
U4(1) - D3(1)E_s^w(1)
\end{bmatrix} \tag{1.32}$$

And finally the solution vector X is:

$$\begin{bmatrix} E_d^w(1) \\ E_d^w(2) \\ E_d^w(3) \\ \ldots \\ E_d^w(k) \\ E_u^w(k) \\ E_u^w(k-1) \\ \ldots \\ E_u^w(2) \\ E_u^w(1) \\ E_u^w(0) \end{bmatrix} \quad (1.33)$$

The above system of equations which represents an analytical solution to the coupled 2 flow irradiance equations can be applied in order to generate synthetic reflectance signatures of optically deep or shallow waters for inhomogeneous media characteristics. In order to simulate the reflectance signatures, specific coefficients based upon the work of Bostater and Gimond[15] and Bostater[16] are utilized as shown in figures 1 and 2 below. Figure 3 and 4 shows the clear water absorption[17] and backscatter coefficients used in calculating the total absorption and total backscatter coefficients using the form of $a=a_w+a_1c_1+a_ic_i$... and $b=b_w+b_1c_1+b_ic_i$... Thus, assumed concentrations of water constituents are used to simulate the magnitudes of total absorption, $a(z,\lambda)$ and backscatter, $b(z,\lambda)$ as a function of wavelength and the water layer depth. Layered model simulations are simulated for 10-meter layer thickness with 5 or 10 layers for a 50 or 100-meter total water column depth. The downwelling light used as input to the model is shown in figure 5 and an atmospheric correction is applied to the solar radiation outside the atmosphere according to Ma[18] and Greg and Carder[19]. The solar radiation entering the water is considered to be composed of collimated direct (sunlight) and diffuse indirect (skylight) as indicated in figure 5. The light entering the water is first modified for the specular and diffuse reflectance and wind roughened surface conditions.

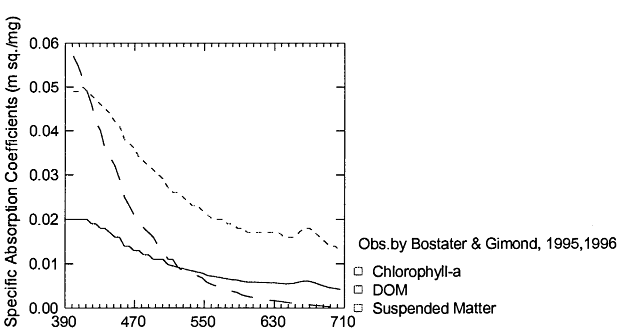

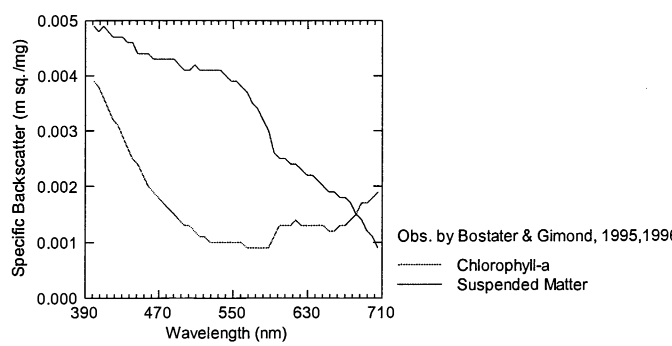

Figures 1-2. Specific absorption and specific backscatter coefficients used for testing and comparing the analytical homogenous model and the layer non-homogeneous model. The data used in calculating these coefficients were collected for waters along Indian River Lagoon, Port Canaveral and the Atlantic Ocean coastal waters off Port Canaveral, Florida.

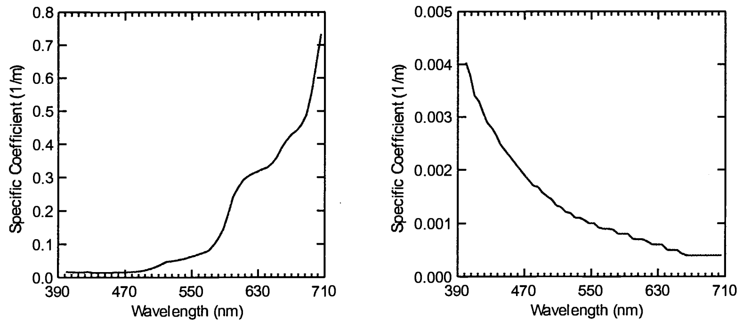

Figure 3 and 4. Pure water absorption and backscatter coefficients used to generate the synthetic layered model hyperspectral signatures of water and for the homogeneous model comparisons.

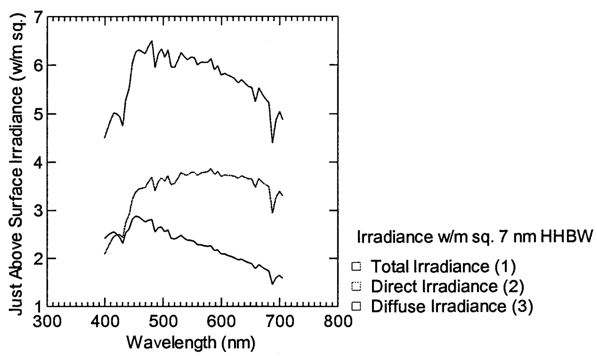

Figure 5 Signatures of the direct and indirect downwelling irradiance used as input into the layered and homogeneous model runs.

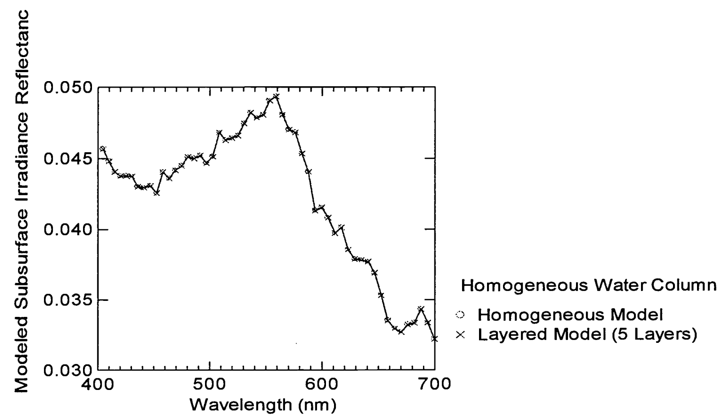

Figure 6. Comparison of the homogeneous and the layered model (5 layers, 50 meter water depth) predicted reflectance signatures for testing the layered model.

3. RESULTS

Figure 6 above shows the preliminary results of comparing the layered model to the homogeneous model. The comparison of the homogeneous and layered (5 layers, 10 m thick layers) analytical solutions above are based upon concentrations of 18 mgL^{-1} seston, 3 mgL^{-1} DOM, 26 ugL^{-1} Chlorophyll-a. Wind speed was assumed at 6 ms^{-1}, and a Caribbean Sea sand bottom type reflectance was used in the hypothetical 50-m water column total depth. Note that comparisons for the mixed water column (homogeneous) simulations indicate nearly exact results at the surface for the 2 model types (homogeneous and layered). The above (figure 6) indicates that the layered model is working as anticipated for simulation the water surface reflectance in waters with constant concentrations of constituents as a function of depth. Figure 7 shows the results of specifying different concentrations of chlorophyll-a in the layered model to determine how this model responds to increasing concentrations. Specifically, this layered model test was simulated in order to determine the difference between the water surface reflectance signatures under different water column concentrations of chlorophyll-a with 10 layers and a total water column depth of 100m. This resulted in signatures similar in nature to the homogeneous model, but once notices the ability to simulate many layers, a bottom type and a deep-water column. Next (figure 9) we simulate a nonhomogeneous water column. This is quite important since in most natural freshwater and coastal water bodies, the concentrations of DOM, suspended particulate matter (seston) and chlorophyll-a pigments vary with from the surface to the bottom. This is especially true in temperature or density stratified waters, or in waters with active primary production within a mixed surface layer. Figure 8 shows the vertical profiles of DOM, chlorophyll-a and seston used and how they varied under two different scenarios. Figure 9 then demonstrates how the results of 2 simulations and specifically, how the water surface reflectance signatures change with depth dependent concentrations of DOM, seston and chlorophyll-a pigment concentrations or water quality variables.

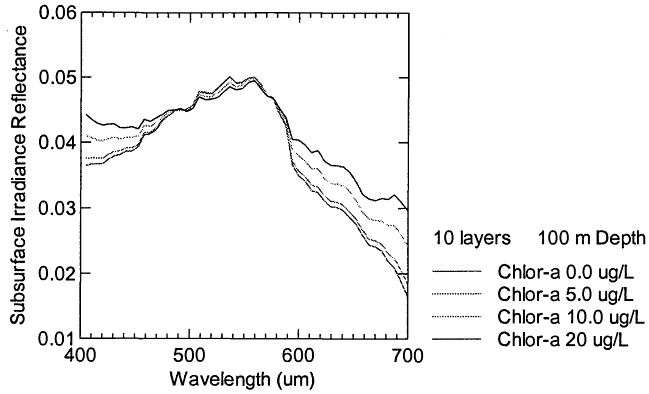

Figure 7. Homogeneous water column concentrations set at 18 mgL^{-1} seston, 3 mgL^{-1} DOM, wind speed 6 m/s, and a sand bottom reflectance. Layered model run was for 10 layers and 100m water depth. Synthetic signatures show the influence of varying chlorophyll-a concentrations.

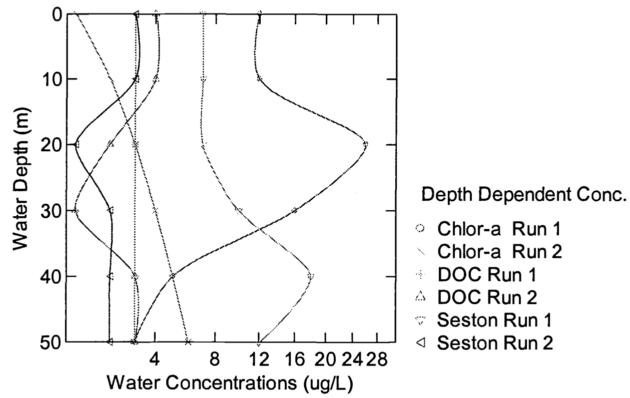

Figure 8. Assumed vertical concentrations of water quality variables for two different model scenarios (Run 1 & Run 2). The layered model was run with 5 layers (10 m layer thickness) for a 50m total water column depth.

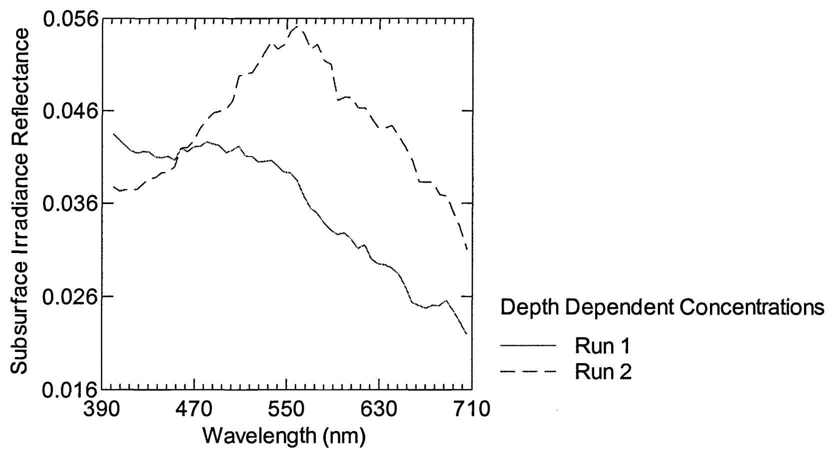

Figure 9. Layered model results indicating the synthetic water surface reflectance simulated as a function of varying the vertical profiles of DOM, seston and chlorophyll-a as indicated in figure 8 for a 5 layer, 50 meter water column depth.

4. DISCUSSION

The above preliminary model results indicate the magnitude of the effect that vertical variations in water column chemical concentrations may have upon measured water surface reflectance signatures. The layered model results suggest that nonhomogeneous characteristics of a water column influences the calculated surface reflectance and thus would affect measured satellite or aircraft based sensor based reflectance, associated imagery, and related algorithms. Future work will be needed to more rigorously test the model and the conservation of energy aspects of the layered model, as well as the effects of different bottom types and methods for calculating the influence of the air-sea interface on the layered model described above.

5. ACKNOWLEGEMENTS

Computers, remote sensing equipment as well as software central to this research has been provided in part by KB Science, and S & C Services. NASA, Kennedy Space Center, Dynamac Corp., US DOE and NSF have assisted in the support of Florida Tech graduate students (M. Gimond, W. Ma, T. McNally, M. Keller, L. Huddleston) and undergraduate student (M. Campbell).

6. REFERENCES

1 Bostater, C., Ma, W., McNally, T., Gimond M., Lamb, A., 1995, "Application of an optical remote sensing model", SPIE Vol. 2586, pp. 32-43.

2 Bostater, C., McNally, T., Ma, W., "Modeling of the underwater light field and its effect on temperature, stability and momentum," SPIE, Vol. 2959, pp. 171-179, 1996.

3 Bostater, C., Ma, W., McNally, T., Gimond M., Lamb, A., "Application of an optical remote sensing model," SPIE, Vol. 2586, pp. 32-43, 1995.

4 Priesendorfer, R., *Hydrologic Optics*, Vol. I-VI, NOAA/ERL, Honolulu, HI, pp.1757, 1978.

5 Petzold, T., "Volume scattering functions for selected ocean waters," SIO Ref. 72-78, In*: Light in the Sea*, Edited by J.E. Tyler, Dowden, Hutchinson & Ross, Stroudsberg, pp. 150-174, 1977.

6 Haltrin, V. L., "Monte Carlo Modeling of Light Field Parameters in Ocean with Petzold Laws of Scattering," 4th Int. Conference on Remote Sensing for Marine & Coastal Environments, Orlando, Florida, pp. 502-508, 1997.

7 Kirk, J.T.O., "Monte Carlo Study of the Nature of the Underwater Light Field in, and the relationship between Optical Properties of, Turbid Yellow Waters," Australian Jrnl. Marine & Freshwater Research. 32, pp. 517-532, 981.

8 Bostater, C., Gimond, M., "Comparing a hyperspectral Monte-Carlo approach for simulating water surface signatures based upon radiative transfer theory: simulating clear water & Caribbean Sea bottom types", SPIE (this volume).

9 Bostater, C., Ma, W., McNally, T., Gimond, M., Lamb, A., "Application of an optical remote sensing model", SPIE, Vol. 2586, pp. 32-43, 1995.

10 P. Kubelka, and F. Munk, "Ein Beitrag zur optik der Farbanstriche," *Z. Tech. Physik* 12, 593, 1931.

11 Bostater, C., "Imaging derivative spectroscopy for vegetation dysfunction assessments", SPIE, Vol. 3499, pp. 277-185, 1998.

12 Morel, A., Prieur, L., "Analysis of variations in ocean colour," Limnology and Oceanography," 22, pp. 709-22, 1977.

13 Kirk, J., *Light and Photosynthesis in Aquatic Ecosystems*, 2nd Edition. Cambridge University Press, 1994.

14 Jerlov, N., *Marine Optics*, Elsevier Oceanography Series, 14, pp. 231, 1976.

15 Bostater, C., Gimond, M., "Methodology evaluation for remotely estimating water quality parameters in estuarine waters", SPIE, Vol. 2586, pp. 14-25, 1995.

16 Bostater, C., "Specific absorption and backscatter coefficient signatures in southeastern Atlantic coastal waters", SPIE, Vol. 3496, pp. 196-200, 1998.

17 Smith, R., Baker, K., "Optical properties of the clearest natural waters, Applied Optics", Vol. 20, pp. 177-184, 1981.

18 Ma, W., "An analytical two-flow model to simulate the distribution of irradiance in coastal waters with a wind – roughened surface and bottom reflectance, Ph.D. Dissertation", Florida Tech, pp. 299, 1997.

19 Greg, W., Carder, K., "A simple spectral solar irradiance model for cloudless marine atmospheres, Limnology & Oceanography", Vol. 35(8), pp. 657-675, 1990.